J Mol Model (2011) 17:2367–2374
DOI 10.1007/s00894-011-0997-4

ORIGINAL PAPER

Molecular dynamics simulations of the folding of poly (alanine) peptides

Peter Palenčár · Tomáš Bleha

Received: 29 October 2010 / Accepted: 26 January 2011 / Published online: 1 March 2011

Abstract The secondary structures and the shapes of long-chain polyalanine (PA) molecules were investigated by all-atom molecular dynamics simulations using a modified Amber force field. Homopolymers of polyaminoacids such as PA are convenient models to study the mechanism of protein folding. It was found that the conformational structures of PA peptides are highly sensitive to the chain length. In the absence of solvent, straight α-helices dominate in short ($n \sim 20$) peptides at room temperature. A shape transition occurs at a chain length n of 40–45; the compact helix-turn-helix structure (the double-leg hairpin) becomes favored over a straight α-helix. For $n=60$, double-leg and the triple-leg hairpins are the only structures present in PA molecules. An exploration of a chain organization in a cubic cavity revealed a clear predisposition of PA molecules for additional breaks in α-helices and the formation of multifolded hairpins. Furthermore, under confinement the hairpin structure becomes much looser, the antiparallel positions of helical stems are disturbed, and a sizeable proportion of the helical stems are transformed from α-helices into 3_{10}-helices.

Keywords Polypeptide · α-Hairpins · Molecular dynamics · Confinement · Chain folding · Self-organization

P. Palenčár · T. Bleha (✉)
Polymer Institute, Slovak Academy of Sciences,
Dubravska cesta 9,
845 41 Bratislava, Slovakia
e-mail: bleha@savba.sk

Introduction

Developments in computational biopolymer science greatly assist our understanding of the mechanism of protein folding. The crucial phases of chain folding in proteins involve the formation of secondary structural elements such as α-helices and β-sheets. Insights into rules governing the assembly of these elements is a key step in elucidating the folding dynamics.

Homopolymers of polyaminoacids are convenient models to study the properties of complex proteins. Computationally, explaining the structural assembly of such synthetic peptides presents a more tractable problem than explaining the folding of proteins. The folding of the best-known representative of the polypeptide group, poly(alanine) (PA), is of considerable interest, as alanine (Ala) is generally viewed as the most helix-stabilizing amino acid residue. Considerable effort [1–8] has been devoted to performing coarse-grained and atomistic simulation studies aimed at understanding the conformational properties of $(Ala)_n$ polymers. For short chains, typically with $n<22$, these computational studies revealed that the abundance of individual secondary structures in Ala peptides at room temperature is significantly affected by the medium [6–8]. The α-helix was verified to be a stable structure of $(Ala)_n$ in vacuum and in a hydrophobic medium, whereas in aqueous solution the extended conformations of the β-type predominated [7, 8].

In a recent study of PA of $n=60$ in vacuum, we reported [9] that the secondary structure of such long-chain Ala peptides is more complex. The preference for helix formation was retained in $(Ala)_{60}$, but instead of straight helices, hairpin-like structures with two and three parallel helical stems were formed. The finding [9] of the formation of compact hairpin-like structures in long-chain PA in vacuum, and presumably in nonpolar media, is directly

relevant to the organization of integral membrane proteins. Such proteins traverse the cell membrane in a zigzag fashion and often fold into α-helical hairpins with antiparallel-oriented strands separated by a short turn. The building block helix-turn-helix is regarded as a supersecondary structural element in integral membrane proteins [10].

As is usual in thermodynamics and kinetics studies of biosystems, the current knowledge of PA secondary structure is based on experiments performed in dilute solutions or on the computer modeling of single molecules. However, the structure and thermodynamics of proteins in a crowded heterogeneous in vivo environment recently attracted a great deal of interest [11–14]. In many situations, the crowding effect due to lipids, nucleic acids, cytoskeletons and other macromolecules in a cellular medium can be mimicked by spatial confinement. Confining a protein to a small inert cage can have significant effect on the unfolding of that protein. It was argued [14] that the unfolded protein state is destabilized by a reduction in the conformational entropy due to confinement-induced exclusion of the more extended structures. The shape and strength of the restricting geometry may lead to considerable changes in the properties of the protein compared to those seen in bulk. The protein's conformation and mobility are particularly affected by restrictions acting in all three dimensions, such as in spherical or cubic cavities.

In the present study we explored the folding of PA peptides in the absence of the solvent via all-atom molecular dynamics (MD) simulations. Two issues relevant to PA in nonpolar, membrane-like media were addressed. Firstly, the secondary structures and the shapes of $(Ala)_n$ molecules of intermediate lengths were examined. We show that at a chain length slightly above $n=40$, the hairpin-like structure of PA becomes favored over the straight α-helix. Secondly, the question of how the helical structure and organization of a PA molecule are affected by its confinement to a cube was explored.

Model and methods

The model and methodology used were described in detail previously [9]. Single molecules $(Ala)_n$ consisting of $n=40$, 45 and 60 Ala residues of the L-form were assumed. The peptides were blocked at the N and C ends by acetyl and methyl amide (NHMe) groups to ensure the charge neutrality of the chain. MD simulations with all atoms treated explicitly were carried out in a canonical NVT ensemble without solvent. A commercial MD package, YASARA [15], was implemented on a parallel computing cluster. In the MD simulations, a PA molecule was placed at the center of a standard cubic simulation cell with dimensions of $x=y=z=25$ nm to speed up the computation of van der Waals interactions using a neighbor search grid. The cell dimensions selected are about 2.8 times the linear dimension of an α-helix of $n=60$ (the contour length $L=8.94$ nm). The molecule was free to translate and rotate. The leap-frog integration algorithm was applied. The temperature was maintained close to the intended value by coupling the system to an external heat bath using a modified version [15] of a Berendsen thermostat with a coupling time constant of 0.1 ps. A strongly fluctuating instantaneous microscopic temperature was not used to change the velocities at each simulation step as in the standard Berendsen thermostat; instead, the time-average temperature was calculated, and then the atom velocities were rescaled [15]. The thermostat is very efficient at relaxing a system to the target temperature, and is suitable for long "unattended" runs. The standard Berendsen thermostat was employed in previous simulations of PA structure as a function of temperature [5, 6].

The Amber-99φ force-field [6] was used in the simulations. This potential was found [6] to be superior to other force fields at reproducing the thermodynamic and kinetic data of PA peptides. Time steps of 0.8 fs and 1.6 fs were selected after trial calculations for the bonded forces (bonds, angles, dihedral angles and planarity) and the long-range forces (electrostatic and van der Waals), respectively. A switching cut-off of 1.4 nm was applied for both electrostatic and van der Waals interactions. The data used to build the MD trajectory were collected every 10 ps during simulations.

The initial structures of the PA for the simulations were generated from an ideal right-handed α-helix by a 10 ns simulation run at high temperatures. In an MD run, the random-coil structure of PA was folded into a helix by slowly decreasing the temperature using a prescribed gradient of a stepwise decrease in temperature (see Fig. 1). The simulation run was divided into a set of constant-temperature sections lasting 10 ns. A variable

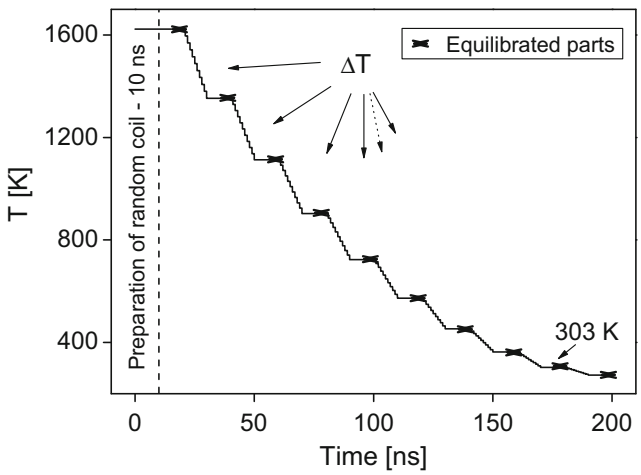

Fig. 1 The simulation protocol of a stepwise decrease in temperature with a variable temperature step ΔT. The preparation phase is also depicted. The *highlighted lines* represent the equilibrated 5 ns parts of the MD runs

temperature step ΔT decreasing from ΔT=270 K at high temperature (1600 K) to ΔT=30 K at 273 K was used. The data were collected from the last 5 ns of the constant-temperature sections. Since the MD runs of 200 ns were carried out for sixteen randomly chosen initial PA structures, the total simulation time for unconfined molecules reached 3.2 μs.

For $(Ala)_{60}$ chains confined to a cube, impermeable walls interacting via a hard plate potential were assumed. The cube side D was expressed relative to the radius of gyration of unconfined PA, D/R_{g0}, where R_{g0}=1.34 nm for $(Ala)_{60}$ at 303 K. By assuming a constant D in a given simulation, seven confinement strengths ranging from large to small cubes were explored. For a given confinement D/R_{g0}, eight 200 ns simulation runs were performed, starting from random initial structures of the PA.

Elements of the secondary structure of PA were assigned according to the DSSP classification [16] based on the grouping of the Ramachandran dihedral angles φ and ψ in the peptide units and an analysis of the H-bond network. The overall helicity H and the number of continuous helical segments N_H were used to quantify the helical structures. The individual helical segments in the PA chain are separated by nonhelical elements such as turns and coils. The distance between the first and the last C_α atoms in the PA chain was used to compute the mean-square end-to-end distance $<R^2>$. Similarly, the mean-square radius of gyration $<R_g^2>$ was calculated using the distances of all C_α atoms from the center of mass. The distribution functions $P(R)$ were evaluated by grouping the respective values of R from the simulations into a histogram. All quantities were calculated as ensemble averages using 4000 values.

Results and discussion

Conversion of the straight α-helix into the α-hairpins

The occurrence of hairpin structures in $(Ala)_{60}$, as reported in [9], is a new phenomenon that was not observed previously in MD simulations of shorter PA molecules. This finding suggests that the conformational structures of PA peptides may be sensitive to not only the environment but also the chain length. It was thus interesting to establish by simulation the minimal length of PA peptide at which the hairpin structure will prevail over the straight α-helix in PA molecules at ambient temperature.

The melting/cooling curve obtained from simulating PA molecules is plotted in Fig. 2. The disordered molecules $(Ala)_n$ where n=40, 45, 60 gradually refold upon cooling into α- and 3_{10}-helices. The overall helicity H of PA at 303 K is about 90%, which is fairly constant for all three

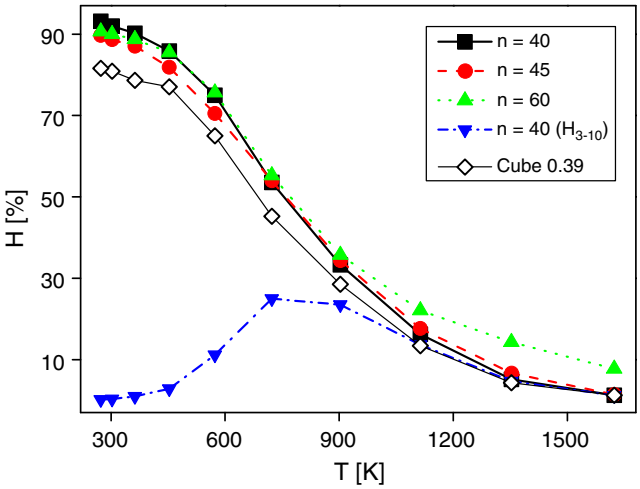

Fig. 2 Temperature dependences of the overall helical contents of free PA chains with n=40, 45, 60 (as specified in the legend) and the n=60 chain confined to a cube at R_{g0}/D=0.39. The fraction of 3_{10}-helices for n=40 is also plotted

chain lengths. The overall helicity H is given by the contributions of three helical types, $H_\alpha + H_{3-10} + H_{PPII}$. In the most common α-helix, H-bonds form between i and i+4 residues. This type of helix is observed almost exclusively in PA at 303 K. The tighter and less frequent structure is the 3_{10}-helix, featuring an H-bonds between i and i+3 residues. Figure 2 shows that the fraction of 3_{10}-helices in PA increases from about zero at 303 K to a maximum of about 25% at 700 K (near to the inflection point of the melting curve); roughly the same fractions are also seen for n=45 and 60 (not shown). The poly(proline) II (PPII) structure of PA is akin to a conformation adopted by poly(proline). In the simulations we found a negligible proportion of such helices.

The high-helicity organization of PA chains can be realized by numerous conformations differing in the number of continuous helical segments N_H. The abundances of structures with a given number of helical segments N_H at 303 K are shown in Fig. 3. It is seen that several distinct forms of the PA molecules coexist in vacuum and in nonpolar media at ambient temperature. Also, there are notable changes in the helical organization of PA as a function of the chain length. In $(Ala)_{60}$, no straight α-helices are detected; instead, the structure with two continuous helical segments (N_H=2) dominates. This structure was identified [9] as the "U" shape configuration of two antiparallel α-helices joined by a small loop region. Figure 3 clearly shows that such a compact structure of PA, termed a two-leg (2 L) α-hairpin, clearly prevails for n=45 as well. The simulation snapshot of this structure is shown in Fig. 4. Nonetheless, besides the 2 L α-hairpins, straight helices of N_H=1 are also present in $(Ala)_{45}$ in an appreciable amount. On the other hand, in a somewhat

shorter molecule, $(Ala)_{40}$, the straight α-helices are much more abundant than the 2 L α-hairpins. Hence, one can infer, in accord with the previous simulations [7, 8], that the straight α-helix is the completely dominant structure in $(Ala)_n$ molecules in a nonpolar medium when $\sim 10 < n < 40$ (approximately). When n is between 40 and 45, a change in the structural preference of PA from the straight α-helix to the 2 L α-hairpin occurs. Moreover, upon increasing the chain length, multifolded hairpins arise in the PA chain. For example, the fraction of three-leg (3 L) α-hairpins (as shown in Fig. 4) increases from zero for $n=40$ to 10.8% for $n=60$ (Fig. 3 and Table 1).

The folding of the straight α-helix into α-hairpins is clearly manifested by the distribution function of the end-to-end distance $P(R)$ of PA molecules at 303 K (Fig. 5). The three leftmost peaks in Fig. 5 correspond to the 2 L α-hairpins in PA chains of various lengths. Obviously, the distance between the chain ends in the U-shaped hairpins is quite small, about $R=0.5$ nm. The two rightmost peaks corresponding to chain-end separations R of about 6 nm and 6.7 nm belong to the straight α-helices for $n=40$ and 45, respectively. One can see that the magnitudes of the 2 L α-hairpin peaks relative to those of the straight helix peaks are about 4:1 for $n=45$ and about 1:4 for $n=40$, in accord with the data in Table 1. Finally, the peak at $R \sim 2.5$ nm, (i.e., in the middle of Fig. 5) corresponds to the 3 L α-hairpin for $n=60$.

A convenient indicator of the shape of a chain molecule is the ratio of the mean-square end-to-end distance to the mean-square radius of gyration. The size ratio $\langle R^2 \rangle / \langle R_g^2 \rangle$ is about 12 for rod-like objects, about 6 for random coils, and of the order of unity for compact objects. The temperature dependences of the computed size ratios plotted in Fig. 6 validate that the PA molecules invariably show random-coil behavior at high temperature. Furthermore, the data for 303 K corroborate that the average shape

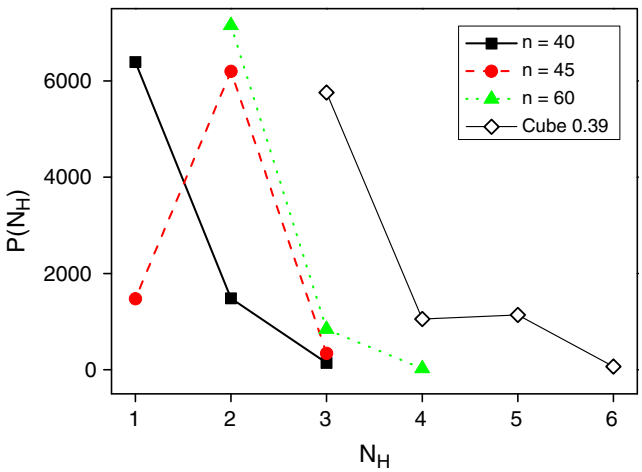

Fig. 3 Distribution functions of the number of continuous helical segments N_H at 303 K in free PA peptides with $n=40$, 45, 60 (as given in the legend) and in PA with $n=60$ confined to a cube at $R_{g0}/D=0.39$

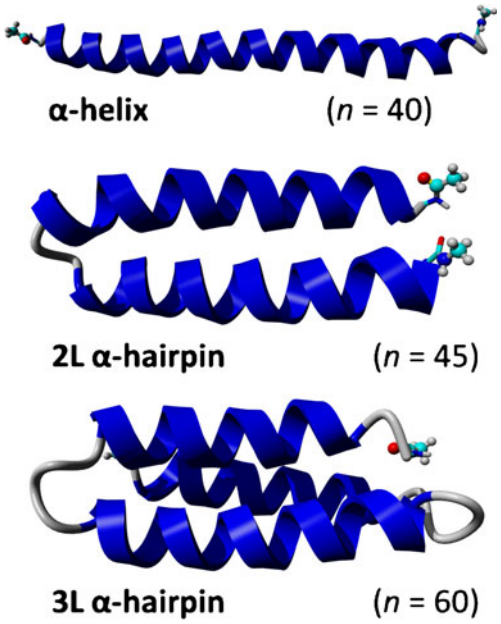

Fig. 4 Simulation snapshots illustrating some typical structural elements of PA chains. The helices are shown as *ribbons*, the nonhelical parts as *tubes*. The straight α-helix is reduced in size by a factor of 0.4 relative to the other two forms. The actual proportions of these structures in a PA of length n is given in Table 1; the bottom 3 L α-hairpin is a minority element

of the PA molecule is greatly modified by the chain length. The rod-like shape of PA predicted for $n=40$ in Fig. 6 is in full agreement with the dominance of the straight α-helix presented in Table 1. Similarly, the low value of the ratio $\langle R^2 \rangle / \langle R_g^2 \rangle$ for $n=60$ in Fig. 6 is a consequence of the very small distances between the chain ends R in the compact hairpin structures. The size ratio of ~5 for $n=45$ follows fwhen the corresponding values for the minority straight α-helix and the majority 2 L α-hairpin structure are averaged.

The depicted transition of PA molecules from a rod-like α-helix into a compact hairpin is intriguing. It is well recognized that in chain molecules, abrupt changes in their shape can be induced by various kinds of stimuli, such as a change in temperature, solvent, pressure, ionic strength, etc. Recently, a shape transition induced by confinement was described for semi-flexible chains in channels and cavities [17]. The case of PA molecules is quite noteworthy considering that the shape transition is triggered by a small change in the length of the molecules.

The driving force for the folding of long-chain PA molecules into hairpins in a nonpolar medium is an attraction between helices. When the chain is sufficiently long, the free-energy penalty for the formation of a disordered loop in a straight helix is surmounted by the attractive energy gained by assuming a hairpin structure. The stabilization energies ΔE of the α-hairpins at 303 K, expressed relative to the corresponding straight α-helix of length n and divided by the number of Ala residues in the

Table 1 Proportions of the different structural forms of $(Ala)_n$ (in %) at 303 K and their relative energies ΔE per PA residue (shown in square brackets; values are in kJ mol^{-1} n^{-1})

n	α-Helix	2 L α-hairpin	3 L α-hairpin	4 L hairpin	5 L
40	79.7 [0]	20.3 [−1.65]	–	–	–
45	18.4 [0]	81.6 [−2.05]	–	–	–
60	–	89.2 [−2.50]	10.8 [−1.35]	–	–
60*	–	–	75.0 [−1.36]	12.5 [0.02]	12.5 [−0.26]

* For PA in a cube of R_{g0}/D=0.39

chain, are listed in Table 1. A comparison of ΔE between the 2 L and 3 L hairpins for n=60 suggests that stability of the folded structures diminishes with the number of folds (hairpin legs). Figure 8 shows the total potential energy ΔE broken down into the individual energy contributions employed in the Amber-99φ force-field [6]. Although the total energy is the primary quantity to consider in the force-field calculations, it is a common approach to use the individual energy terms in a qualitative analysis, particularly when considering the difference between two conformations [4]. Qualitatively, the Coulomb and VdW terms have a clear physical origin. However, the other force-field terms for bonded interactions are somewhat artificial and are presented in Fig. 7 for the sake of completeness. It is seen in Fig. 7 that the van der Waals energy term ΔE_{VdW} makes a major contribution to the total stabilization energy. All other energy terms are smaller and show a trend for mutual compensation. As the PA molecules become shorter, the stabilization energy ΔE per residue (as well as its contributions) diminishes slightly. For PA molecules that are longer than n=40–45, which show a preference for α-hairpins over straight α-helices, the energy analysis suggests that the van der Waals attraction between optimally packed antiparallel α-helices is largely responsible for the folding of PA helices.

The finding of compact hairpin-like structures in long-chain PA is significant for investigations of various helix-forming peptides and for membrane protein modeling. The study of Ala-rich peptides, with a high content (~90%) of Ala residues, greatly enhanced our understanding of the stability of α-helices [18, 19]. Recent experiments [18] using the small-angle X-ray scattering technique revealed that the α-helix is much less rigid and less resistant to being broken than usually thought. As a result, the Ala-rich α-helical peptides behave as somewhat compact semi-broken rods rather than straight cylindrical rods [18]. In a related paper [19], the mechanism of folding of Ala-rich peptide Fs-21 (composed of 21 residues) was investigated by MD in water using the implicit solvent approach. Among the numerous conformations detected, the helix-turn-helix structure was found to be the favored one at 300 K in water. This hairpin-like structure was stabilized mainly by hydrophobic interactions. The compact hairpin-like structures observed in our simulations of PA peptides in vacuum closely resemble the organization of integral membrane proteins. Proteins traverse the cell membrane in a zigzag fashion and fold in the form of stacked α-helices. Transmembrane α-helices vary considerably in length, typically ranging from 15 to 40 residues long.

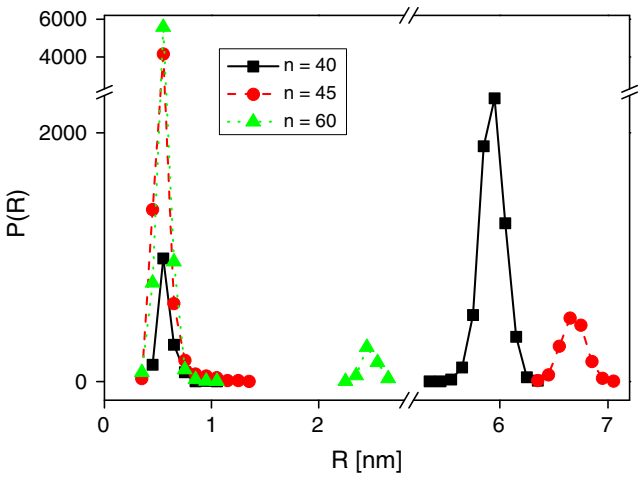

Fig. 5 Distribution functions for the end-to-end distances $P(R)$ of PA molecules with lengths n=40, 45, 60 (as given in the legend)

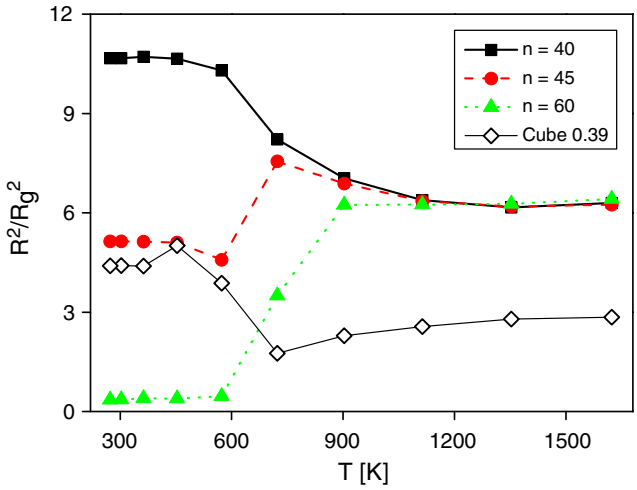

Fig. 6 Temperature dependence of the size ratio $<R^2>/<R_g^2>$ for free PA chains with lengths n=40, 45, 60 (as given in the legend) and a PA chain with n=60 confined to a cube at R_{g0}/D=0.39

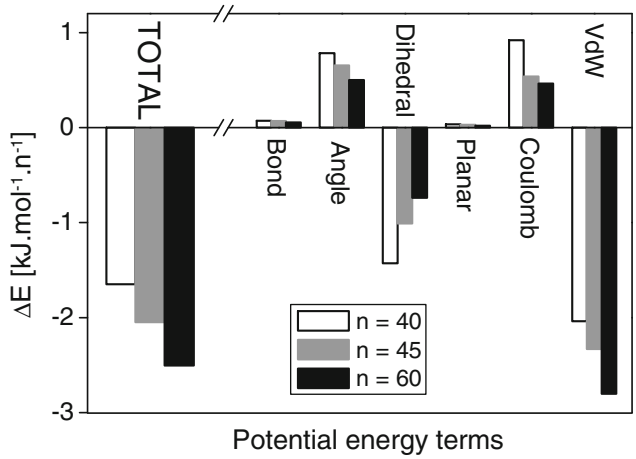

Fig. 7 Difference ΔE between the potential energy of the 2 L α-hairpin and that of the corresponding straight α-helix of the same length n. Individual contributions to the potential energy are labeled

The upper limit of this range coincides fairly well with the critical PA molecule length required for compact α-hairpins to dominate over rod-like α-helices, as established in our simulations.

PA peptide in a cubic cavity

Confining a PA molecule to a small inert cavity can have a significant effect on the folding equilibrium. The results for $(Ala)_{60}$ chains confined to a cube are presented below. The confinement strength is expressed as the ratio of the cube's size to the radius of gyration of the unconfined molecule, D/R_{g0}, or by its inverse value R_{g0}/D. A radius R_{g0}=1.34 nm was computed for $(Ala)_{60}$ at 303 K. The variations in the overall helicity H and its components H_α and H_{3-10} with the confinement strength R_{g0}/D are presented in Fig. 8. Practically no effect is discernible with weak confinement. For moderate confinement, a reduction in the overall helicity takes place. This actually involves an even larger drop in the fraction of α-helices but an increase in the fraction of 3_{10}-helices (up to the value of about 16%). Very strong

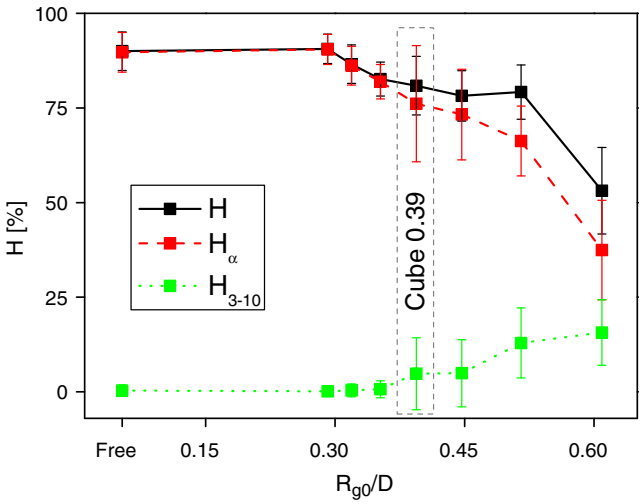

Fig. 8 Dependence of the overall helical fraction and the fractions of α-helices and 3_{10}-helices on the confinement strength R_{g0}/D of $(Ala)_{60}$ in the cube at 303 K. The moderate confinement region R_{g0}/D=0.39 addressed in the analysis is highlighted

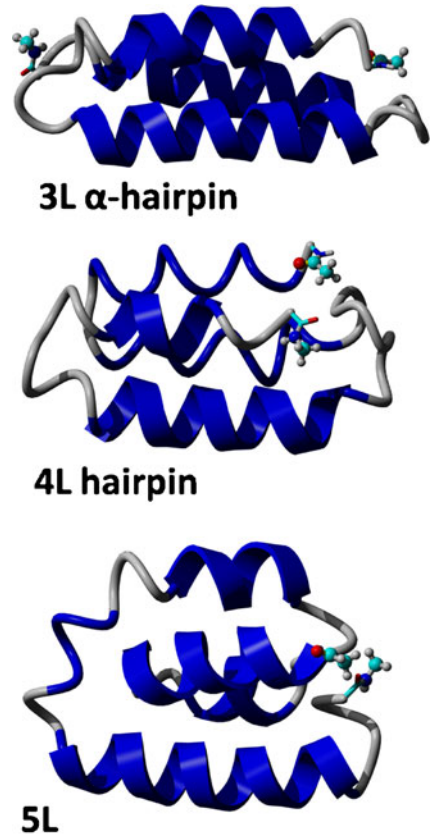

Fig. 9 Hairpin-like structures of PA specific to cubic confinement with R_{g0}/D=0.39. The α-helices are shown as *ribbons*, the 3_{10}-helices as *tubes of the same color*, and nonhelical parts as *bright tubes*

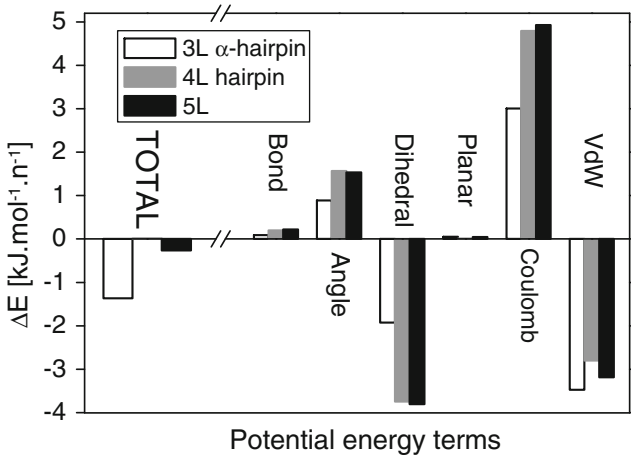

Fig. 10 Potential energy differences ΔE (relative to the corresponding straight α-helix) of the hairpin-like structures of PA under confinement (see Fig. 9). Individual contributions to the potential energy are labeled

confinement with R_{g0}/D=0.61 brings about a significant reduction in the overall helicity H~50% (Fig. 8). Such behavior implies extensive confinement-induced melting of PA helices into disordered structures. In the following we will focus on characterizing the $(Ala)_{60}$ structure for moderate confinement (R_{g0}/D=0.39).

The melting curve of the PA molecule in the cube at R_{g0}/D =0.39 is shown in Fig. 2. The overall helicity H is slightly reduced relative to free chains. Accordingly, the folding pattern shown in Fig. 4 for the free chains should change for the PA molecule confined in the cube. Such confinement-induced modification of the secondary structure of PA is highlighted by a comparison of the number of continuous helical segments N_H between PA (n=60) in a free space and in the cube (Fig. 3). Instead of 2 L α-hairpins, the 3 L α-hairpin is the most abundant structure of PA in the cube at 303 K. Moreover, two additional structures with N_H=4 and N_H=5 are present in the cube to a considerable extent.

The hairpin-like structures of PA at 303 K found in simulations of the cube with R_{g0}/D=0.39 are depicted in Fig. 9. The images represent the simulation snapshots that were compatible (within ±10%) with the average values of the quantities H, R and N_H. The 3 L α-hairpin in a cube, which is practically identical to the equivalent structure in free chains, is displayed in Fig. 9, together with two extra hairpin-like structures observed under confinement. The 4 L hairpin involves four helical stems: two of the α-helix type (in the forefront in Fig. 9) and two of the 3_{10}-helix type (at the back in Fig. 9). The average end-to-end distance of this structure is R~0.7 nm. The 5 L structure with N_H=5 and of R~0.5 nm, which distantly resembles the hairpin, involves four parallel, mostly α-helical stems and one short 3_{10}-helix oriented almost perpendicular to the four others.

An examination of the nature of the hairpin-like structures of PA in the cubic cavity using the data in Fig. 3 and Fig. 9 and the distribution functions of the end-to-end distance $P(R)$ (not shown) allow the identification of two effects that arise due to confinement. First, new short breaks occur within the helical stems (legs) of the 2 L and 3 L α-hairpins. As a result, the number of continuous helical segments N_H increases, meaning that it is no longer identical to the number of legs in a hairpin. Furthermore, the antiparallel position of the helical stems is perturbed by these breaks (the 5 L structure in Fig. 9). Second, a sizeable fraction of the helical stems in the hairpins are transformed from α-helices into 3_{10}-helices (the 4 L hairpin and 5 L structure in Fig. 9). The 3_{10}-helix is thinner and more flexible than the α-helix and so is better adapted to being squeezed under confinement.

The potential energies of three hairpin-like structures of PA shown in Fig. 9 are presented in Fig. 10. The most abundant conformation in the cube is the 3 L α-hairpin. Its energy ΔE per residue, −1.36 kJ mol^{-1} n^{-1}, is practically identical to that in free space (Table 1). The remaining two conformations in the cube, the 4 L hairpin and 5 L, show much smaller stabilization energies and thus much smaller and similarly abundant populations (Table 1). A breakdown of the total potential energy ΔE in the cube into components (Fig. 10) is somewhat different from that derived for a free PA molecule (see Fig. 7).

Conclusions

The folding of $(Ala)_n$ peptides in the absence of solvent was examined via all-atom MD simulations. It was found that conformational structures of PA peptides are highly sensitive to not only the medium but also the chain length. In vacuum and in a nonpolar medium, straight α-helices dominate in short (n~20) peptides at room temperature. For chain lengths $n$of40–45, a shape transition occurs such that the compact double-leg hairpin structure becomes favored over the straight α-helix. For n=60, double-leg and triple-leg hairpins are the only structures present in PA molecules. Upon examining the helical organization of PA molecules in a cubic cavity, an increase in the number of breaks in helical segments and an inclination to form multi-leg hairpins was found under moderate confinement. Under strong confinement, a considerable reduction in the overall helicity of PA molecules was observed because the helical chains melt due to packing requirements. The described self-organization of long PA molecules into compact structures resembles the organization of integral membrane proteins into stacked α-helices. The typical length of a protein α-helix traversing a membrane is comparable to the critical length of a PA molecule at which helical rods break into α-hairpins.

Acknowledgments This work was supported by the Science and Technology Assistance Agency under contract nos. APVV-0079-07 and No. APVV-0607-07, and by VEGA grants 2/6116/26 and 2/6014/26. The work also benefited from the Centers of Excellence Program of the Slovak Academy of Sciences (COMCHEM).

References

1. Smith AV, Hall CK (2001) α-Helix formation: discontinuous molecular dynamics on an intermediate-resolution protein model. Proteins 44:344–360
2. Shental-Bechor D, Kirca S, Ben-Tal N, Haliloglu T (2005) Monte Carlo studies of folding, dynamics, and stability in α-helices. Biophys J 88:2391–2402
3. Mortenson PN, Evans DA, Wales DJ (2002) Energy landscapes of model polyalanines. J Chem Phys 117:1363–1377
4. Nymeyer H, Garcia AE (2003) Simulation of the folding equilibrium of α-helical peptides: a comparison of the generalized born approximation with explicit solvent. Proc Natl Acad Sci USA 100:13934–13939

5. Garcia AE (2004) Characterization of non-alpha helical conformations in Ala-peptides. Polymer 45:669–676
6. Sorin EJ, Pande VS (2005) Exploring the helix-coil transition via all-atom equilibrium ensemble simulations. Biophys J 88:2472–2493
7. Levy Y, Jortner J, Becker OM (2001) Solvent effects on the energy landscapes and folding kinetics of polyalanine. Proc Natl Acad Sci USA 98:2188–2193
8. Soto P, Baumketner A, Shea J-E (2006) Aggregation of polyalanine in a hydrophobic environment. J Chem Phys 124:134904–134910
9. Palencar P, Bleha T (2010) Folding of polyalanine into helical hairpins. Macromol Theory Simul 19:488–495
10. Khutorsky V (2003) Alpha-hairpin stability and folding of transmembrane segments. Biochem Biophys Res Commun 301:31–34
11. Zhou HX (2008) Protein folding in confined and crowded environments. Arch Biochem Biophys 469:76–82
12. Cheung MS, Klimov D, Thirumalai D (2005) Molecular crowding enhances native state stability and refolding rates of globular proteins. Proc Natl Acad Sci USA 102:4753–4758
13. Sikorski A, Romiszowski P (2007) Computer simulation of polypeptides in a confinement. J Mol Model 13:327–333
14. Lucent D, Vishal V, Pande VS (2007) Protein folding under confinement: a role for solvent. Proc Natl Acad Sci USA 104:10430–10434
15. Krieger E, Darden T, Nabuurs S, Finkelstein A, Vriend G (2004) Making optimal use of empirical energy functions: force-field parameterization in crystal space. Proteins 57:678–683
16. Kabsch W, Sander C (1983) Dictionary of protein secondary structure: pattern recognition of hydrogen-bonded and geometrical features. Biopolymers 22:2577–2637
17. Cifra P, Bleha T (2010) Shape transition of semi-flexible macromolecules confined in channel and cavity. Eur Phys J E 32:273–279
18. Zagrovic B, Jayachandran G, Millett IS, Doniach S, Pande VS (2005) How large is α-helix? Studies of the radii of gyration of helical peptides by small-angle X-ray scattering and molecular dynamics. J Mol Biol 353:232–241
19. Zhang W, Lei H, Chowdhury S, Duan Y (2004) Fs-21 peptides can form both single helix and helix-turn-helix. J Phys Chem B 108:7479–7489